Vol. 628: 223–234, 2019
https://doi.org/10.3354/meps13113

MARINE ECOLOGY PROGRESS SERIES
Mar Ecol Prog Ser

Published October 10

Identifying foraging habitats of adult female long-nosed fur seal *Arctocephalus forsteri* based on vibrissa stable isotopes

Dahlia Foo[1,*], Mark Hindell[1], Clive McMahon[2], Simon Goldsworthy[3]

[1]Institute for Marine and Antarctic Studies, University of Tasmania, Hobart, Tasmania 7004, Australia
[2]Sydney Institute of Marine Science, Mosman, New South Wales 2088, Australia
[3]Aquatic Sciences Centre, South Australian Research and Development Institute, West Beach, South Australia 5024, Australia

ABSTRACT: We investigated how foraging ecotypes of female long-nosed fur seals *Arctocephalus forsteri* could be identified from vibrissa stable isotopes. We collected regrowths of vibrissae from adult females (n = 18) from Cape Gantheaume, Kangaroo Island, South Australia, from 2 breeding seasons (2016, 2017). The period represented by the regrowth was known, and 8 individuals were administered with ^{15}N-enriched glycine as a biomarker to mark the start date of the regrowth. Non-glycine-marked and glycine-marked vibrissae were used to estimate the rate of the individual vibrissa regrowth. Using individual growth rates (0.18 ± 0.04 mm d^{-1}), we reconstructed a stable isotope (δ^{13}C and δ^{15}N) time series for each regrowth and allocated them to corresponding at-sea locations either based on geolocation tracks (n = 14) or foraging habitat type (shelf or oceanic) based on diving data (n = 2) of the sampled seals. Mean (±SD) δ^{15}N from vibrissa segments was higher when females foraged on the continental shelf region (16.1 ± 0.7‰, n = 29) compared to oceanic waters (15.1 ± 0.7‰, n = 106) in 2017, whereas it was similar in both regions in 2016 (shelf: 15.3 ± 0.4‰, n = 13; oceanic: 15.4 ± 0.4‰, n = 15). Based on the stable isotope signatures of vibrissa segments, model-based clustering analysis correctly classified 79.8% as originating from shelf or oceanic foraging habitats. This demonstrates the potential of using vibrissa stable isotopes for studying the foraging ecology of an important top marine predator.

KEY WORDS: Isoscape · Foraging strategies · Trophic dynamics · Continental shelf · Oceanic · Marine top predators

1. INTRODUCTION

Marine predators, including pinnipeds, whales, sharks and seabirds, play an important role in ecosystem structure and function (Camphuysen 2006, Estes et al. 2011). The spatial and temporal variability of their foraging behaviour can influence prey populations and fisheries interactions and can indicate the consequences of human-induced changes to the marine environment (Boyd & Murray 2001, Reid & Croxall 2001). An important aspect for foraging ecology is understanding how individuals adapt their foraging strategies (such as feeding location and prey type) in response to intra- and inter-annual changes in prey availability and quality. This is especially relevant for animals foraging in the highly dynamic marine environment.

Naturally occurring stable isotopes of carbon (^{13}C) and nitrogen (^{15}N) in marine environments are good indicators of habitat source and consumer trophic level within food webs, respectively (Ramos & González-Solís 2012). Ratios of ^{15}N/^{14}N (δ^{15}N) can indicate a consumer's trophic position as ^{15}N is enriched along the food chain (Crawford et al. 2008). In the southern hemisphere, ratios of ^{13}C/^{12}C (δ^{13}C) of marine plankton show broad-scale geographical

*Corresponding author: dahlia.foo@utas.edu.au

gradients that increase from the equator with latitude to the subtropics before decreasing with latitude in the Southern Ocean (Francois et al. 1993, Trull & Armand 2001, Cherel et al. 2007). Similarly, $\delta^{13}C$ also varies from inshore/benthic to offshore/pelagic food sources, generally decreasing from coastal to offshore areas (Hobson et al. 1994). As $\delta^{13}C$ values vary little along the food chain, they can be used to indicate a consumer's habitat (Crawford et al. 2008). However, habitat information obtained from $\delta^{13}C$ values are broadscale at most, and oftentimes need to be validated with location data (Newsome et al. 2010). Combining tracking information with stable isotopes allows a more thorough investigation of foraging ecology (Lowther et al. 2013, Walters et al. 2014, Jeanniard-du-Dot et al. 2017). As diet is the primary contributor of an animal's isotopic composition (Peterson & Fry 1987), stable isotopes are increasingly being used to investigate foraging ecology, including individual variability in foraging strategies (Kernaléguen et al. 2012, Baylis et al. 2016), ontogeny (Chaigne et al. 2013, Vales et al. 2015), migration patterns (Best & Schell 1996, Walters et al. 2014, Dannecker 2016) and diet (Cherel et al. 2008, Jeanniard-du-Dot et al. 2017).

Various animal tissues have different isotopic turnover rates, which influences the inferential timescale of isotopic data. Keratinous tissues such as vibrissae (whiskers) of pinnipeds have a turnover rate that integrates isotopic information over a scale of days to weeks (Cherel et al. 2009). This means that for otariids, which do not shed their vibrissae periodically (as opposed to phocids, which do) (Hirons et al. 2001, Newland et al. 2011), vibrissae provide a time series of historical information that can date back on average 4–5 (up to 8) yr (Kernaléguen et al. 2015, Rea et al. 2015). Additionally, sampling vibrissae is logistically easier and less costly than using biologgers for studying certain aspects of foraging ecology, thus allowing for greater sample sizes.

To accurately obtain a time series of isotopic information from vibrissae, 2 types of information are required: vibrissa growth rates and the length of the vibrissa segment analysed. One method of 'time stamping' stable isotope signatures in vibrissae is to administer a ^{15}N-enriched glycine, which is incorporated into the vibrissa keratin, thereby providing a temporal marker. Thus, the administration date of ^{15}N-enriched glycine would appear as a spike in the $\delta^{15}N$ results of sequentially sampled segments along a vibrissa, enabling growth rate calculations (Hirons et al. 2001, Tyrrell et al. 2013).

The goal of this study was to validate if vibrissae isotope values can be used to infer foraging ecotypes of female long-nosed fur seals *Arctocephalus forsteri* (LNFS). LNFS are common in southern Australia, where they are important top predators within the Great Australian Bight ecosystem. The Great Australian Bight is important for fishing, aquaculture and ecotourism industries (Rogers et al. 2013). One of the major breeding colonies of LNFS is located at Cape Gantheaume, Kangaroo Island. During the breeding season and subsequent lactation period, adult females provision a single pup onshore. These females forage from this central place, typically feeding on the continental shelf during the austral summer coastal upwelling period (January–April), switching to feeding in oceanic waters in late autumn to winter (mid-April–September), when the upwelling activity ceases (Baylis et al. 2008, Foo et al. 2019). While the seasonal changes in foraging habitat of lactating LNFS are fairly well documented (Foo et al. 2019), our understanding of individual inter-annual variability in their foraging behaviour is still limited. Tracking and measuring the foraging behaviours of the same individuals over multiple years using biologgers can be challenging; however, the use of vibrissa stable isotopes may be a way of solving this problem. Specifically, we aimed to (1) quantify individual vibrissa growth rates, (2) quantify temporal and spatial variability of $\delta^{13}C$ and $\delta^{15}N$ from vibrissae and (3) identify stable isotopic niches and evaluate the extent to which they reflect the observed switch between shelf and oceanic foraging.

2. MATERIALS AND METHODS

2.1. Study site, animal handling and instrumentation

The study was undertaken between February 2016 and September 2017 at Cape Gantheaume (36° 04′ S, 137° 27′ E), Kangaroo Island, South Australia (Foo et al. 2019). In late summer (February–March), 18 lactating female LNFS (2016 n = 5, 2017 n = 13) were randomly selected and captured using a hoop net. Upon capture, anaesthesia was induced and maintained using Isoflurane (Veterinary Companies of Australia), administered via a portable gas anaesthetic machine (Stinger™, Advanced Anaesthesia Specialists). Anaesthetised seals were weighed (±0.5 kg) and their body length (nose to tail) and axillary girth were measured (±1 cm). Miniature time–depth recorders (TDR) (Lotek; 2016: LAT1800L, 36 × 11 × 17 mm,

10 g; 2017: LAT1800SFP, 36 × 11 × 8 mm, 5.4 g) and solar geolocation (global location sensor; GLS) tags (Intigeo-C330, Migrate Technology; 17 × 19 × 8 mm, 3.3 g) were deployed on all female seals via attachment on the flipper tag following Arthur et al. (2015). The TDRs recorded depth every 1 s. GLS recorded ambient light and temperature from which twice-daily locations were estimated. A vibrissa was also cut as close to the seal's cheek as possible. In 2017, 12 of the tagged females were also administered with glycine enriched in ^{15}N isotope (98%; Novachem). This was done by subcutaneous injection into the fat layer of the belly as a solution of 100 mg ml^{-1} in sterile physiological saline at a dosage of approximately 5 mg glycine kg^{-1} of body mass (Hirons et al. 2001). Glycine was used to timestamp the vibrissa due to the high mole percentage of glycine found in vibrissa keratin (Hirons et al. 2001). In winter, tagged females were recaptured, the GLS loggers were recovered, and the regrown vibrissa were collected by (1) again cutting as close to the cheek as possible in 2016 and (2) plucking to include the root in 2017 (Fig. 1). In addition to the regrown vibrissa, a new vibrissa was plucked at the same time in both years; however, these were not used in this study.

2.2. Sample preparation and stable isotope analyses

Vibrissae were washed in deionised water, cleaned with successive rinses in a 2:1 chloroform:methanol solution and then dried in an oven at 60°C for 48 h. The vibrissae were then weighed and sectioned into approximately 2 mm segments. Starting from the base, the segments from each vibrissa were numbered sequentially. The segments were packed in tin containers, and the relative abundance of ^{13}C and ^{15}N were determined using an Isoprime (Micromass) continuous-flow isotope-ratio mass spectrometer. Stable isotope concentrations were expressed in standard δ notation: $\delta X=(R_{sample}/R_{standard}-1)\times1000$, where X is ^{13}C or ^{15}N and R is the corresponding ratio, i.e. ^{13}C:^{12}C or ^{15}N:^{14}N. $R_{standard}$ is the Pee Dee Belemnite for $\delta^{13}C$ and atmospheric N_2 (air) for $\delta^{15}N$. The units are expressed in parts per thousand (‰). Stable isotope analysis was performed by the Central Science Lab, University of Tasmania, Hobart, Australia. Precision of measurements are ±0.1‰ SD for both $\delta^{13}C$ and $\delta^{15}N$. A total of 47 standards were used for carbon and nitrogen, where a new standard was typically used after every 10th sample. Nitrogen standards used included ammonium sulphate and L-glutamic acid. Carbon standards included limestone, graphite and L-glutamic acid.

The regrown vibrissa consisted of the subcutaneous section of the vibrissa at the date of the first cut (pre-study information) along with the actual regrowth, which reflects information generated during the study period (Fig. 1). We assumed that the length of the subcutaneous section of the vibrissa was constant at both vibrissa sampling occasions. Because the regrown vibrissae was sampled differently in both years (cut in 2016; plucked in 2017), the length of the regrowth section for 2016 equalled the length from base to tip of the vibrissa, while the vibrissae lengths plucked in 2017 equalled the length from base to tip minus the length of the subcutaneous section (Fig. 1).

Individual vibrissa growth rates are expressed in mm d^{-1} and were calculated by the equation:

$$\text{length of regrowth / duration between } t_1 \text{ and } t_2 \quad (1)$$

where t_1 is the date of the first cut and t_2 is the date when the regrowth was re-sampled. The glycine

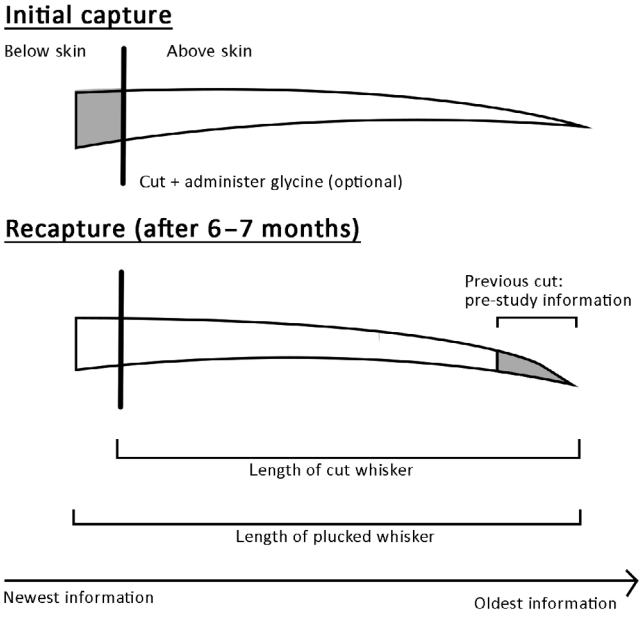

Fig. 1. Schematic of how vibrissa regrowths from individual female long-nosed fur seals were obtained at recapture. During the initial capture, all vibrissae were cut; however, only some animals were administered ^{15}N-enriched glycine as a biomarker to time stamp the initial capture. A portion from the tip of the vibrissa at recapture contained pre-study information. The unshaded portion of the vibrissa at recapture represents the actual regrowth with information from the study period. The length of the pre-study portion of the vibrissa was assumed to be the same length as the subcutaneous length of the vibrissa sample. At recapture, regrowths from individuals in 2016 and 2017 were cut and plucked, respectively. Most recent information is located at the base. Not drawn to scale

marker causes a sharp increase in $\delta^{15}N$ values, indicating its injection date. Thus, the vibrissa growth rate for glycine-injected seals was also calculated by the equation:

base to spike length / days since injection (2)

Using individual vibrissa growth rates, corresponding dates were estimated for each vibrissa segment starting from the final sampling date (i.e. base). For the cut vibrissa regrowths, we accounted for the missing subcutaneous section (newest information) by measuring that of the plucked vibrissaes that were sampled at the same time. For glycine-injected seals, the vibrissa growth rate calculated using the glycine spike was used for estimating dates, since it was more accurate than the alternative. If the glycine spike covered more than one vibrissa segment, the earliest segment was assigned to the injection date (i.e. initial capture date).

We used data from the glycine-injected seals to estimate the potential error in date estimation using individual vibrissa growth rates calculated from the regrowth length (Eq. 1). To do this, we calculated the difference between the actual injection date (as indicated by the glycine spike) and the estimated injection date (t_1) obtained from the vibrissa growth rate calculated from Eq. (1). To ensure consistency, subsequent analyses were done using the vibrissa growth rates obtained from Eq. (1) for all seals.

2.3. Statistical analyses

All data analyses were done using R v.3.5.1 (R Core Team 2017). Raw light data from the GLS loggers allowed us to obtain 2 location estimates d^{-1} during deployment, which were divided into individual foraging trips (details in Foo et al. 2019). The accuracy of the geolocation estimates was 45 ± 29 km (Foo et al. 2019). In areas with higher prey density, we would expect longer residence time associated with periods of area-restricted search, and hence a proxy for foraging effort (Dragon et al. 2010, Pistorius et al. 2017). Thus, the cell residence time in each 30 km grid cell was calculated for each foraging trip using the 'trip' package in R (v.1.5.0; Sumner 2016). The size of the grid cell was chosen to account for the error associated with GLS tags while still providing a realistic representation of true locations. Trips with <3 locations and locations within a 10 km buffer around the colony were removed. Core foraging areas were determined as those in the 90th percentile of the cell residence time for each foraging trip. Each trip was then classified as 'shelf' (including continental shelf and shelf break; bathymetry ≤2000 m) or 'oceanic' (bathymetry >2000 m), depending on the furthest point of that foraging trip from the colony. If the corresponding location data were not available for a seal's vibrissa stable isotope data, we inferred that the seal foraged exclusively on shelf or oceanic waters, or both, from associated unpublished diving data if they were available. Typically, the maximum depths of dives are distinct between shelf (~100 m) and oceanic foraging (~200 m). We matched vibrissa segments to the core foraging cells of the nearest foraging trip for each individual by comparing the estimated date of each vibrissa segment and the median date of foraging trips. By restricting vibrissa segments to trip-level we avoided matching them to a date that happened to correspond to a location during the transit phase of a foraging trip. While this means that the isotopic data of individual vibrissae segments may represent periods of transit and feeding in a given foraging trip, stable isotopes assimilated into an animal's tissue occur mainly from foraging.

Since all the vibrissa regrowths contained pre-study period information, segments with estimated dates prior to the first capture date of the seal were removed from further analyses. Additionally, $\delta^{15}N$ values that were influenced by glycine were excluded from further analyses, but their corresponding $\delta^{13}C$ values were still included. To compare stable isotopes between shelf and oceanic habitats, we used a model-based clustering approach (based on $\delta^{13}C$ and $\delta^{15}N$ values) using the package 'Mclust' (v.5.4.4; Fraley & Raftery 2007). In this approach, a clustering model that allows for overlapping clusters with varying geometric properties and quantifies the uncertainty of observations belonging to clusters is estimated for the data. Model selection was made using Bayesian information criteria because this method commonly penalises overly complicated models.

To investigate the relationship between latitude and stable isotope ($\delta^{13}C$ and $\delta^{15}N$) values, we fitted generalised additive mixed models with Gaussian distributions and identity links for each stable isotope, with trip nested within individuals as random effects and the 2-way interaction between year and latitude as smoothed terms. Autocorrelation and heterogeneity issues were addressed by specifying a first-order autocorrelation structure and/or power variance function, respectively. Linear mixed models were fitted separately for each stable isotope against the interaction between region and year and the

interaction between region and breeding state (provisioning vs. unconstrained; see Section 3.3), with trip nested within individual as a random effect. All model selections were done using a backward selection process where Akaike's information criterion (AIC) was used to assess model performance where appropriate; models with a better fit have lower AIC values. All *t*-tests were 2-tailed, and if values did not fulfil normality assumptions the non-parametric Wilcox *t*-test was used. Significance of statistical tests was assessed at the 0.05 level; mean values are given ±SD.

3. RESULTS

3.1. Stable isotope and foraging habitat data

We recaptured and obtained regrowth vibrissae from 18 females across both study years. Three of the recaptured individuals had lost their GLS loggers and the GLS data from one individual was corrupted, leaving the remaining 14 with corresponding GLS tracks. Two of the individuals without GLS data had dive data recorded up to May (not shown). A summary of the vibrissa sampling process and the types of data obtained from individuals is shown in Table 1. A total of 306 vibrissa segments were obtained with an average of 17.3 ± 4 segments ind.$^{-1}$. The average length of the subcutaneous section for plucked vibrissae was 8.7 ± 1.1 mm (Table 1). The average length of cut and plucked vibrissa regrowths were 34.8 ± 11.2 and 36.7 ± 7.3 mm, respectively. Out of those possible vibrissa segments, 18 were lost during the process of sectioning and 13 subcutaneous segments of plucked vibrissae were excluded because their isotope values were anomalous (Hückstädt et al. 2012). Pre-study whisker segments were also excluded from the analysis, leaving a total of 222 segments. Of that number, 18 segments were influenced by glycine and hence their $\delta^{15}N$ information was also removed from further analyses. Overall, 204 vibrissa segments had complete $\delta^{13}C$ and $\delta^{15}N$ information. Of those segments, 151 corresponded with GLS-derived core foraging areas and 12 corresponded with foraging habitat information derived from dive data during the study period.

Table 1. Details of 18 adult female long-nosed fur seals whose vibrissa regrowths were sampled and if they had simultaneous data from geolocation sensor (GLS) or time–depth recorder (TDR) tags. Four individuals were not provisioning a pup and hence were considered unconstrained to central place foraging. Some individuals were also administered ^{15}N-enriched glycine on the capture date to biologically mark the date. Individual vibrissa growth rates were calculated using 2 methods: with or without using the spike in ^{15}N from the glycine biomarker (see Section 2.2 for details). Foraging habitats were determined from biologger data (more details of vibrissa lengths in Table S1 in the Supplement)

ID	Capture date (A)	Recapture date	Provisioning a pup?	Glycine	Growth rate (mm d^{-1}) Without glycine	With glycine	Estimated injection date (B)	B – A (d)	GLS	TDR	Foraging habitats
2016											
69	26-Feb	19-Sep	Y		0.23						
71	5-Feb	27-Aug	Y		0.23						
73	1-Feb	22-Aug	Y		0.13				Yes		Shelf/oceanic
77	5-Feb	21-Aug	Y		0.14				Yes		Shelf/oceanic
450	16-Feb	25-Sep	Y		0.12				Yes		Shelf/oceanic
2017											
307	29-Jan	4-Aug	N		0.16				Yes		Oceanic
311	5-Feb	7-Aug	Y		0.17				Yes		Shelf/oceanic
329	12-Feb	25-Jun	Y		0.17					Yes	Oceanic
340	14-Feb	18-Jul	N		0.17				Yes		Oceanic
353	13-Mar	29-Jun	Y		0.21				Yes		Oceanic
315	6-Feb	6-Jul	Y	Yes	0.16	0.19	29-Jan	–8	Yes		Shelf
317	7-Feb	7-Aug	N	Yes	0.25	0.27	4-Feb	–3	Yes		Oceanic
318	7-Feb	29-Jun	Y	Yes	0.13	0.14	15-Feb	8		Yes	Shelf
319	7-Feb	5-Jul	Y	Yes	0.22	0.25	2-Feb	–5	Yes		Shelf/oceanic
322	9-Feb	12-Jul	Y	Yes	0.18	0.19			Yes		Shelf/oceanic
324	10-Feb	11-Jul	N	Yes	0.18	0.15			Yes		Oceanic
326	10-Feb	7-Aug	Y	Yes	0.18	0.16	19-Mar	37	Yes		Shelf/oceanic
351	13-Feb	30-Jun	Y	Yes	0.18	0.17	2-Mar	17	Yes		Oceanic
Overall mean					0.18 ± 0.04	0.19 ± 0.05		7.7 ± 17.1			

3.2. Vibrissa growth rates

The threshold for identifying the glycine spike was $\delta^{15}N > 17.6‰$, which generally consisted of 1–4 vibrissa segments (Fig. S1 in the Supplement at www.int-res.com/articles/suppl/m628p223_supp.pdf). Using growth rates of glycine-marked vibrissae, on average the estimated glycine injection date was 7.6 ± 17.1 d later than the actual glycine injection date (Table 1). This calculation was done excluding 2 of the glycine-marked seals which had missing data covering the entire duration of the glycine spike. The average vibrissa growth rates, calculated with and without using the glycine spike as a reference, were 0.18 ± 0.04 and 0.19 ± 0.05 mm d^{-1} (Wilcox test: $W = 64$, p = 0.68), respectively.

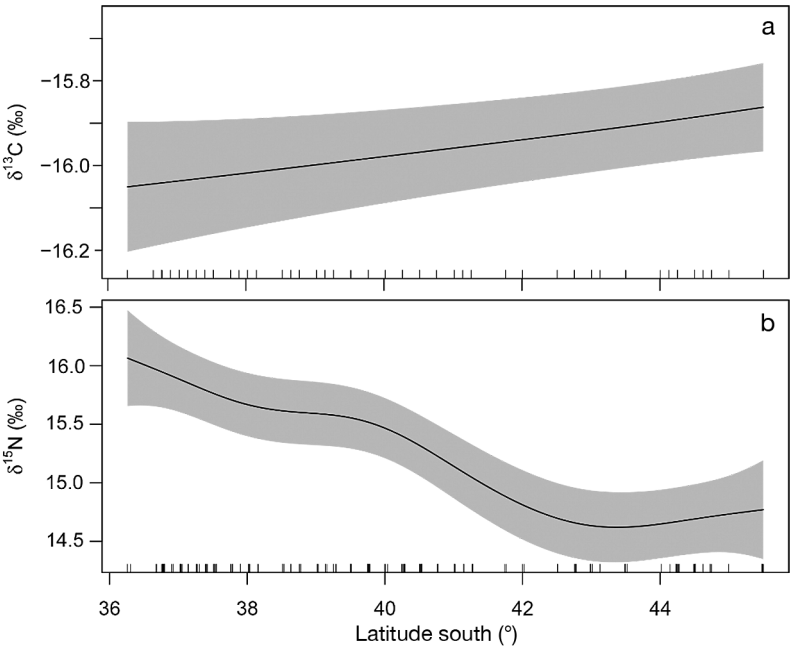

Fig. 2. Smoothed effects of latitude on (a) carbon and (b) nitrogen stable isotopes from female long-nosed fur seals for 2017 as determined by generalised additive models. Shaded area: ±2 SE

3.3. Spatial and temporal variability in vibrissae isotope ratios

The number of foraging trips per individual ranged from 5–22 (mean = 11.4 ± 5.5). The average duration of each foraging trip was 10.6 ± 8.8 d. The cell residence time in a core foraging 30 × 30 km cell ranged from 8–136.3 h (mean = 27 ± 14.2 h). Core foraging areas primarily occurred on the distal portion of the track (Fig. S2). Four individuals did not display central place foraging behaviour, which might have been due to either pup abandonment or their pup dying; hence we considered these females unconstrained (Table 1).

Generalised additive mixed models revealed that $\delta^{13}C$ increased, while $\delta^{15}N$ decreased, with increasing latitude. These relationships were only significant for 2017 (Figs. 2 & S3, Table 2). In total, 66.4% of individual trips (obtained from GLS data) had one vibrissa segment assigned to them (range = 1–4). Because sample sizes per individual trip were small, trip was not used as a nested random effect within individual seals in mixed models. From the 16 seals that had all or some corresponding foraging habitat information (from GLS or TDR data; Table 1), 42 and 121 vibrissa segments were assigned to shelf and oceanic habitats, respectively. $\delta^{13}C$ was influenced by habitat (shelf vs. oceanic) where $\delta^{13}C$ was lower on the shelf (Fig. 3a, Table 3). The final model for $\delta^{15}N$ included the breeding state of females and the interaction between year and habitat (Table 3). $\delta^{15}N$ values of provisioning females were greater than unconstrained females (Fig. 3b). The effect of habitat on $\delta^{15}N$ differed between years, whereby $\delta^{15}N_{shelf}$ was slightly lower than $\delta^{15}N_{oceanic}$ in 2016 and $\delta^{15}N_{shelf}$ was greater than $\delta^{15}N_{oceanic}$ in 2017 (Fig. 3c, Table 3). Unconstrained females were generally smaller in length (128 ± 5.6 cm) than females provisioning pups (136 ± 6.6 cm; Welch 2-sample *t*-test: $t = 2.55$, df = 5.69, p = 0.0457).

3.4. Variability of isotopic niches among individuals

Model-based clustering revealed that segments of individual adult female vibrissa regrowths during the

Table 2. Approximate significance of smooth (*s*) terms from generalised additive models. Statistically significant terms are in **bold**

Term	edf	ref.df	*F*-statistic	p
$\delta^{15}N$ ~ *s*(latitude, by = year)				
s(latitude):year2016	1	1	1.44	0.23
***s*(latitude):year2017**	**4.21**	**4.21**	**17.13**	**0.00**
$\delta^{13}C$ ~ s(latitude, by = year)				
s(latitude):year2016	1.05	1.05	3.82	0.05
***s*(latitude):year2017**	**1.39**	**1.39**	**5.54**	**0.02**

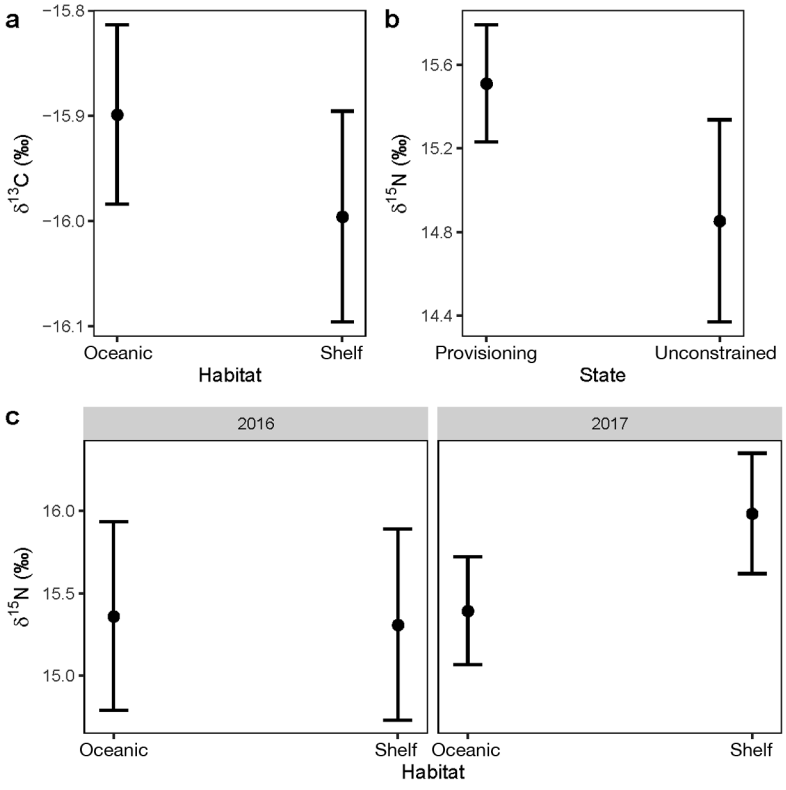

Fig. 3. Effect of (a) habitat on $\delta^{13}C$, (b) breeding state on $\delta^{15}N$ and (c) conditional effect of habitat on $\delta^{15}N$ depending on year for female long-nosed fur seals. Error bars: confidence intervals

lactation period could be separated into 3 clusters represented by ellipses that encompassed distinct isotopic niches (Fig. 4). The uncertainty in the classification ranged from 0.005–49.6%, with 75% (n = 153) of our samples having an uncertainty of 14.5% or less. One of the clusters was primarily associated with shelf foraging (cluster 2) while the other 2 were primarily associated with oceanic foraging (clusters 1 and 3; Fig. 4). Out of 163 vibrissae samples, 79.8% were correctly classified into an oceanic or shelf cluster based on their stable isotope signature. Misclassified samples were primarily located between cluster ellipses, had high uncertainty and corresponded to the shelf break region where points from different clusters overlapped (Fig. 4b). No stable isotope samples from 2016 were allocated to cluster 2 (Table S3). Between the oceanic clusters (1 and 3), cluster 3 had higher $\delta^{15}N$ and $\delta^{13}C$ values and the spatial range of those values was similar (Fig. 4b).

After obtaining the cluster groups, we were interested in investigating the relationship between oceanic clusters (1 or 3) and the interaction between year and day-of-the-year (based on the estimated date for each vibrissae segment). Cluster 2 (shelf) was not considered since it had a relatively small sample size (n = 20). Using a logistic mixed model, with the same model selection process as described in Section 2.3, we found that the probability of being in cluster 3 increased with increasing date for both years, but that the rate of change in probability was greater in 2016 (Fig. 5, Table 3). A summary of individual and cluster stable isotope values is shown in Table S4.

4. DISCUSSION

Our study contributes to the literature on vibrissa growth rates in pinnipeds (Hirons et al. 2001, Kernaléguen et al. 2012, McHuron et al. 2016, Chilvers 2019). Few other studies have used $\delta^{15}N$-enriched glycine to estimate the growth rates of otariid vibrissae (Hirons et al. 2001, de Lima et al. 2019). By combining the vibrissae stable isotopic and geolocation data, we have shown that the broad-scale foraging habitats (i.e. shelf vs. oceanic clusters) of female LNFS can be identified based on bulk

Table 3. Statistical summaries of the final models. $\delta^{13}C$ and $\delta^{15}N$ were fitted as linear mixed models with a Gaussian link. The oceanic cluster model was a logistic mixed model with a logit link. For results of model selection process see Table S2

Term	Effect	Estimate	SE	*T*-statistic
$\delta^{15}N$				
(Intercept)	Fixed	15.36	0.29	52.8
Regionshelf	Fixed	−0.05	0.19	−0.27
Year2017	Fixed	0.03	0.34	0.1
Stateunconstrained	Fixed	−0.66	0.29	−2.28
Regionshelf:year2017	Fixed	0.64	0.24	2.7
Seal (intercept) SD	Random	0.45		
Residual SD	Random	0.49		
$\delta^{13}C$				
(Intercept)	Fixed	−15.9	0.04	−369
Regionshelf	Fixed	−0.1	0.04	−2.37
Seal (intercept) SD	Random	0.15		
Residual SD	Random	0.18		
Oceanic cluster				
(Intercept)	Fixed	−6.68	2.8	−2.38
Yday	Fixed	0.12	0.04	2.7
Year2017	Fixed	6.32	3.14	2.01
Yday:year2017	Fixed	−0.1	0.04	−2.23
Seal (intercept) SD	Random	1.75		

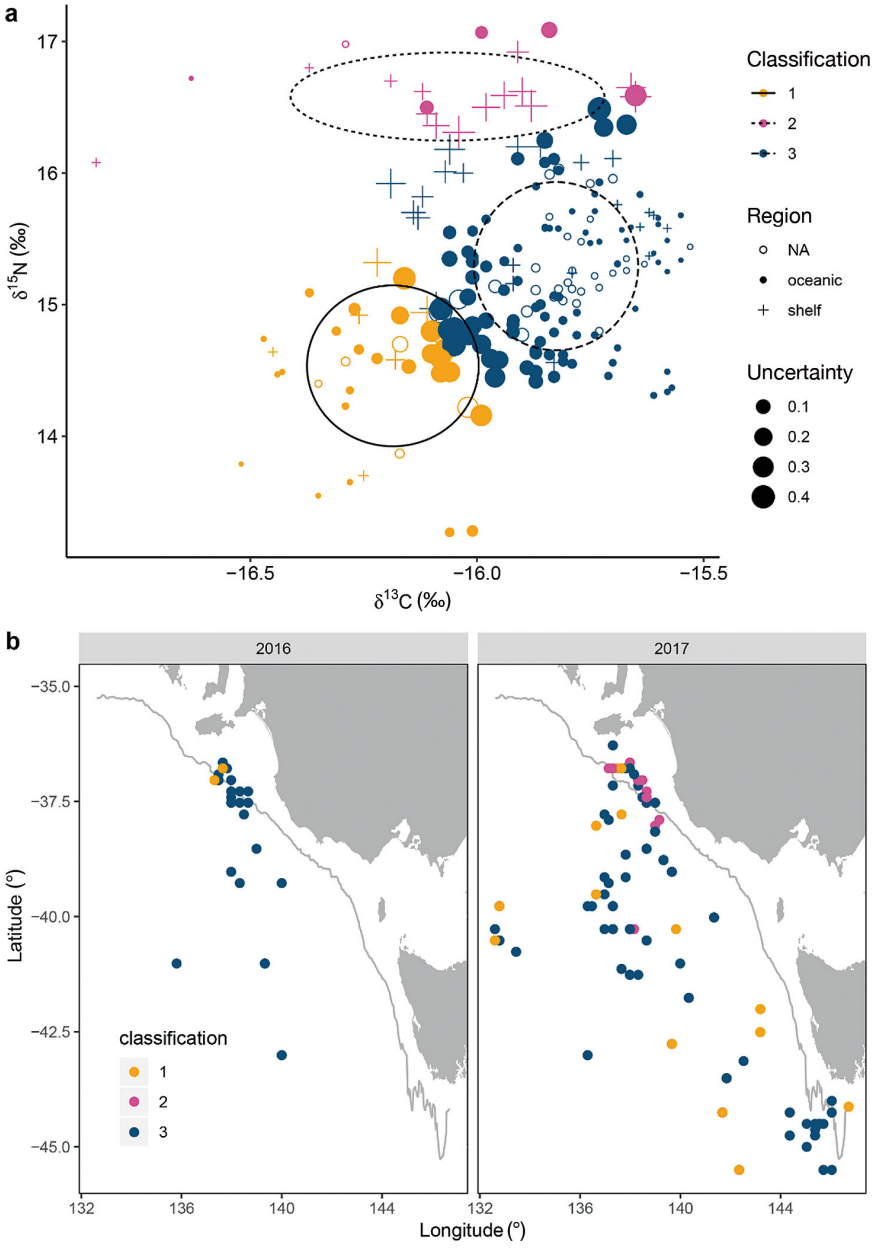

Fig. 4. Isotope biplots (a) of $\delta^{15}N$ and $\delta^{13}C$ values for lactating long-nosed fur seal vibrissa sampled from Cape Gantheaume. Each data point represents the stable isotopic composition of a segment that was sampled sequentially along each vibrissa. Using individual estimated vibrissa growth rates, we reconstructed a stable isotope time series from each vibrissa and matched them to corresponding foraging locations (shelf vs. oceanic) obtained from geolocation tags or time–depth recorders. NA: Vibrissa segments without corresponding foraging region information; do not appear as data points in (b). Ellipses surrounding data points: significant clusters derived from model-based cluster analysis, with data points from the same cluster represented by the same colour. The size of data points represented relative classification uncertainty by the cluster analysis where larger symbols indicate less certain observations. (b) Spatial map of core foraging areas (each point is the median core foraging location of a trip) distinguished by their classification group and by year. Grey line: 2000 m isobath separating continental shelf and shelf break from oceanic waters

nitrogen and carbon stable isotopes. Thus, vibrissae stable isotope signatures show potential for distinguishing different foraging strategies of adult females (i.e. oceanic or shelf only or both, or unconstrained; Fig. S4) and fidelity to foraging sites (i.e. diversity of isotopic niches), which can affect their reproductive performance in different years (Bradshaw et al. 2004).

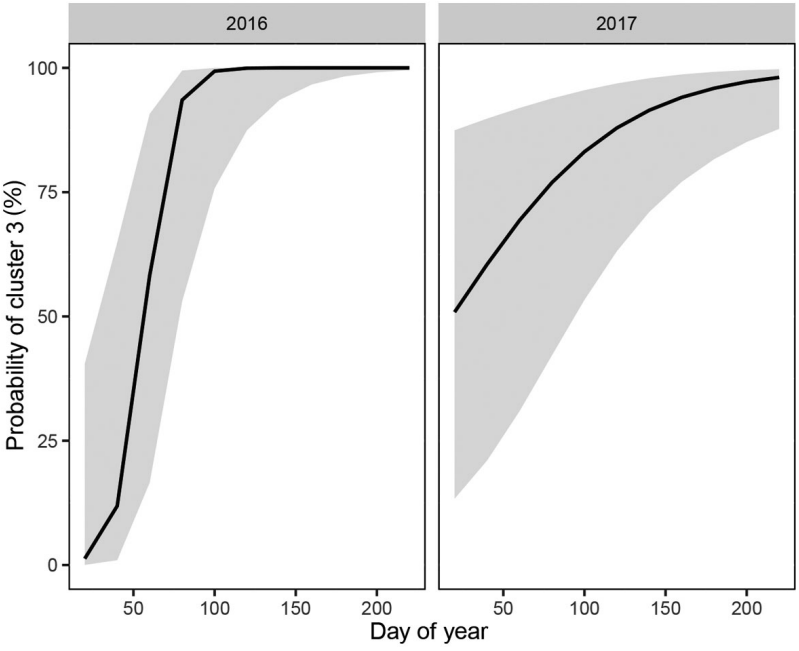

Fig. 5. Interaction effect between day-of-the-year and year on the probability of a female long-nosed fur seal vibrissae stable isotope sample being in cluster 3 (as opposed to cluster 1). Both cluster groupings were obtained from model-based clustering analysis and are primarily associated oceanic foraging. Shaded area: confidence intervals of the model

4.1. Vibrissae growth rates

The vibrissae growth rates obtained without the use of the glycine marker are minimum estimates, as we did not take into account potential wear at the tip of vibrissae (Rea et al. 2015, McHuron et al. 2019). Nevertheless, the mean vibrissae growth rates calculated with (0.19 mm d^{-1}) and without (0.18 mm d^{-1}) glycine were similar, thus providing support for the accuracy of our results. Furthermore, stable isotope information at the tip of the regrown vibrissa would have corresponded to pre-study information, which was not used in this study. This study's vibrissae growth rates were comparable to those of other otariids such as wild subadult and adult Stellar sea lions *Eumetopias jubatus* (0.1–0.17 mm d^{-1}, glycine method; Hirons et al. 2001) and adult male Antarctic fur seals *Arctocephalus gazella* and subantarctic fur seals *A. tropicalis* (both 0.14 mm d^{-1}), but were more than twice that of female Antarctic (0.08 mm d^{-1}) and subantarctic (0.09 mm d^{-1}) fur seals (Kernaléguen et al. 2012). The differences in vibrissae growth rates among species and animal sizes indicates that caution should be taken when referencing vibrissae growth rates of other species in analyses.

4.2. Spatial variability of stable isotope ratios

Variation in carbon ratios is generally influenced by sea surface temperatures (SSTs) with lower $\delta^{13}C$ in cooler waters, producing a broad latitudinal gradient where $\delta^{13}C$ decreases towards the poles (Trueman et al. 2012). However, in the southern hemisphere, this negative relationship between $\delta^{13}C$ and latitude is more prominent south of the subtropical convergence zone (~42° S). North of this zone the correlation between $\delta^{13}C$ and latitude is positive (Best & Schell 1996, Bax et al. 2001, Trull & Armand 2001). This is likely due to other factors that can influence particulate organic matter (POM) $\delta^{13}C$ such as plankton growth rates, cell geometry and taxonomy (Trueman et al. 2012). This is consistent with our results which showed a positive correlation between $\delta^{13}C$ and latitude. Additionally, the mixing of shelf waters with carbon-depleted waters from the subtropical front that spill onto the shelf in association with upwelling events in summer and the carbon-depleted eastward flowing Leeuwin Current off Western Australia at the start of winter may lead to lower $\delta^{13}C$ on the shelf (Lowther et al. 2013). Furthermore, Australia has an extensive northern boundary ocean system where cross-shelf exchange of water (Middleton & Bye 2007) may transport relatively carbon-enriched coastal waters off the shelf via more mobile mid-trophic level animals, thus in turn enriching the $\delta^{13}C$ values of the adjacent oceanic waters.

The mixing of different water masses due to the unique geographical characteristics of our study region may also explain our relatively low range of $\delta^{13}C$ values (1.2‰). In comparison, Bax et al. (2001) reported that the range of $\delta^{13}C$ from 37–45° S for their study was ~4‰. The $\delta^{13}C$ POM values obtained by Bax et al. (2001) were taken from oceanic waters within the Indian Ocean, whereas the relatively small spatial range in our study may have been influenced by the inshore/offshore $\delta^{13}C$ gradient (where $\delta^{13}C$ generally decreases offshore) as well as the broader $\delta^{13}C$ latitudinal gradient. The small $\delta^{13}C$ range likely also contributed to the misclassification of some data points between shelf and oceanic clusters. There may not always be a clear difference in $\delta^{13}C$ between inshore and offshore habitats due to the combined ef-

fects of biological and physical properties of the local area, including currents and food web structure (Hansen et al. 2012). It is also possible for stable isotope signatures of zooplankton communities within different water types (i.e. shelf vs. oceanic warm- and cold-core eddies) to be similar, which would contribute towards overlapping shelf and oceanic stable isotope signatures (Henschke et al. 2015). Compound-specific stable isotope analysis (Crawford et al. 2008, Lorrain et al. 2009) would be useful in finding out the baseline values of $\delta^{13}C$ and $\delta^{15}N$ in different water types and hence their origin for accurate comparison.

The ranges of $\delta^{13}C_{shelf}$ (−16.8 to −15.6‰) and $\delta^{15}N_{shelf}$ (13.7 to 16.9‰) overlapped with those obtained from the vibrissa of a sympatric male Australian sea lion *Neophoca cinerea* ($\delta^{13}C$: mean = −17.6‰, range = −18.7 to −16.2‰; $\delta^{15}N$: mean = 15.5‰, range = 15.2 to 16‰), which forages on the continental shelf year-round in the same region (Lowther et al. 2013). The range of $\delta^{15}N_{shelf}$ is greater for female LNFS than male Australian sea lions, which may suggest the former group is consuming a wider range of prey than the latter. However, a direct comparison of stable isotope values between different species and sexes may not be entirely accurate since their trophic discrimination factors may differ slightly (Jenkins et al. 2001). Nonetheless, Australian sea lions are benthic foragers (Lowther et al. 2013), whereas LNFS are pelagic foragers (Page et al. 2005); the lower range of $\delta^{13}C_{shelf}$ of the Australian sea lion may reflect benthic foraging since $\delta^{13}C$ tends to be lower in cooler waters and with increasing depth (Kroopnick 1985).

Prey consumed in the different habitats may have been different between years. In 2017, prey consumed during shelf foraging trips had a higher $\delta^{15}N$ than prey consumed during oceanic foraging trips. This likely explains why unconstrained females, which forage more frequently in oceanic waters, generally had lower $\delta^{15}N$ than provisioning females. Conversely, in 2016 $\delta^{15}N$ was very similar between both habitats, suggesting that the diet composition of females, particularly on the shelf, can vary interannually (i.e. proportion of each prey type) or that there was a shift in $\delta^{15}N$ at the base of the food web between years (Ruiz-Cooley et al. 2014). The primary diet of female LNFS on the shelf includes red bait, jack mackerel and Gould's squid, whereas in oceanic waters it is primary myctophids (e.g. lantern fish) (Baylis et al. 2009). If the former reason was true, the higher $\delta^{15}N$ on the shelf in 2017 may have been due to females consuming more shelf prey with higher $\delta^{15}N$ such as Gould's squid (Fig. S5). The increased consumption of relatively low-energy benthic fish and cephalopods (higher $\delta^{15}N$) may have been driven by relatively weaker upwelling on the shelf in 2017 (Foo et al. 2019). If variability in $\delta^{15}N$ in our study was instead due to baseline $\delta^{15}N$ variability between years, it would mean that the mean trophic level of prey that females are consuming in their respective habitats may actually be the same in different years after accounting for baseline $\delta^{15}N$ shifts.

4.3. Identifying foraging strategies based on clusters

There was a relatively strong isotope signature for the shelf (Fig. S4), as represented by cluster 2. This may be useful as a baseline reference for foraging strategies used by lactating LNFS, i.e. shelf-only foraging during the pup-rearing period is represented by a minimum threshold of −16.8 and 16.1‰ for $\delta^{13}C$ and $\delta^{15}N$, respectively. Interestingly, cluster 2 was only found in 2017, which suggests that the trophic landscape in 2016 somehow led to more similar foraging behaviour and that cluster 1 and/or 3 also include shelf foraging isotope signatures. This may explain the lack of distinction between shelf and oceanic stable isotope signatures (especially $\delta^{15}N$) in 2016, which may have been due to oceanic prey also occurring on the continental shelf slope and outer shelf water and/or the extent to which females foraged on the shelf during the transit phase of their oceanic foraging trips.

Nevertheless, clusters 1 and 3 also occurred in the oceanic region far away from the continental shelf, which suggests that there were different groups of oceanic prey. One possible explanation is that females may encounter various frontal and eddy features which may have different stable isotopic signatures that can also change over time (Henschke et al. 2015). Indeed, oceanic cluster 3, which generally had higher $\delta^{13}C$ and $\delta^{15}N$ than oceanic cluster 1, was associated with foraging later in the year and when females spent more time foraging. There is high eddy activity within the oceanic region, especially in winter (D. Foo et al. unpubl. data), and the subtropical front region has a high incidence of eddy formation and eddy shedding (Tomczak et al. 2004). The $\delta^{13}C$ and $\delta^{15}N$ values of a warm-core (anticyclonic) eddy can increase significantly after a phytoplankton bloom induced by upwelling (Henschke et al. 2015). Warm-core eddies may also have higher $\delta^{13}C$ than cold-core (cyclonic) eddies. The different stable isotopic signatures between eddy types is a reflection of the type of zooplankton community (Waite et al. 2007) which may attract different types of prey.

4.4. Conclusion

The isoscape generated from stable isotope analysis of LNFS vibrissae shows relatively high spatial variability, which may be characteristic of this region as a result of complex biophysical processes on the shelf and in oceanic waters. However, using biogeomarkers from vibrissae regrowths may still allow us to broadly distinguish between shelf and oceanic foraging locations and hence the type of individual foraging strategy (shelf or oceanic only foraging, or both). Future studies may consider analysing complete vibrissae to identify annual cycles in stable isotopes to further verify vibrissae growth rates (Kernaléguen et al. 2012). Additionally, vibrissae of pups may also be used to assess within- and between-population variability in maternal alternate foraging strategies (Scherer et al. 2015, Baylis et al. 2016), including individual foraging fidelity to foraging locations between years.

Acknowledgements. This study was supported through grants from the Sea World Research and Rescue Foundation, the Holsworth Wildlife and Research Endowment, and the Lirabenda Endowment Fund (issued by the Field Naturalists Society of South Australia). All animal handling was undertaken with the approval from the Primary Industries and Regions South Australia animal ethics committee (application 32-12), Department of Environment, Water and Natural Resources (permit A24684) and the University of Tasmania animal ethics committee (permit A0015176). We thank A. Walters for providing her expertise in stable isotope analyses and for the helpful discussions on this work. We also thank the 3 reviewers who helped improve the manuscript tremendously.

LITERATURE CITED

Arthur B, Hindell M, Bester M, Trathan P and others (2015) Return customers: foraging site fidelity and the effect of environmental variability in wide-ranging Antarctic fur seals. PLOS ONE 10:e0120888

Bax NJ, Burford M, Clementson L, Davenport S (2001) Phytoplankton blooms and production sources on the south-east Australian continental shelf. Mar Freshw Res 52:451–462

Baylis AMM, Page B, Goldsworthy SD (2008) Effect of seasonal changes in upwelling activity on the foraging locations of a wide-ranging central-place forager, the New Zealand fur seal. Can J Zool 86:774–789

Baylis AMM, Hamer DJ, Nichols PD (2009) Assessing the use of milk fatty acids to infer the diet of the Australian sea lion (*Neophoca cinerea*). Wildl Res 36:169–176

Baylis AMM, Kowalski GJ, Voigt CC, Orben RA, Trillmich F, Staniland IJ, Hoffman JI (2016) Pup vibrissae stable isotopes reveal geographic differences in adult female southern sea lion habitat use during gestation. PLOS ONE 11:e0157394

Best P, Schell D (1996) Stable isotopes in southern right whale (*Eubalaena australis*) baleen as indicators of seasonal movements, feeding and growth. Mar Biol 124:483–494

Boyd IL, Murray AWA (2001) Monitoring a marine ecosystem using responses of upper trophic level predators. J Anim Ecol 70:747–760

Bradshaw CJA, Hindell MA, Sumner MD, Michael KJ (2004) Loyalty pays: potential life history consequences of fidelity to marine foraging regions by southern elephant seals. Anim Behav 68:1349–1360

Camphuysen CJ (2006) Top predators in marine ecosystems: their role in monitoring and management. Cambridge University Press, Cambridge

Chaigne A, Authier M, Richard P, Cherel Y, Guinet C (2013) Shift in foraging grounds and diet broadening during ontogeny in southern elephant seals from Kerguelen Islands. Mar Biol 160:977–986

Cherel Y, Hobson KA, Guinet C, Vanpe C (2007) Stable isotopes document seasonal changes in trophic niches and winter foraging individual specialization in diving predators from the Southern Ocean. J Anim Ecol 76:826–836

Cherel Y, Ducatez S, Fontaine C, Richard P, Guinet C (2008) Stable isotopes reveal the trophic position and mesopelagic fish diet of female southern elephant seals breeding on the Kerguelen Islands. Mar Ecol Prog Ser 370:239–247

Cherel Y, Kernaléguen L, Richard P, Guinet C (2009) Whisker isotopic signature depicts migration patterns and multi-year intra- and inter-individual foraging strategies in fur seals. Biol Lett 5:830–832

Chilvers B (2019) Whisker stable isotope values indicate long-term foraging strategies for female New Zealand sea lions. Endang Species Res 38:55–66

Crawford K, McDonald RA, Bearhop S (2008) Applications of stable isotope techniques to the ecology of mammals. Mammal Rev 38:87–107

Dannecker DJ (2016) Comparing stable isotope values from vibrissae of newborn Antarctic fur seal pups (*Arctocephalus gazella*) to those of their mothers to better understand adult female foraging ecology and migration patterns. MSc thesis, University of California, San Diego, CA

de Lima RC, Franco-Trecu V, Vales DG, Inchausti P, Secchi ER, Botta S (2019) Individual foraging specialization and sexual niche segregation in South American fur seals. Mar Biol 166:1–12

Dragon AC, Monestiez P, Bar-Hen A, Guinet C (2010) Linking foraging behaviour to physical oceanographic structures: southern elephant seals and mesoscale eddies east of Kerguelen Islands. Prog Oceanogr 87:61–71

Estes JA, Terborgh J, Brashares JS, Power ME and others (2011) Trophic downgrading of planet earth. Science 333:301–306

Foo D, McMahon C, Hindell M, Goldsworthy S, Bailleul F (2019) Influence of shelf oceanographic variability on alternate foraging strategies in long-nosed fur seals. Mar Ecol Prog Ser 615:189–204

Fraley C, Raftery AE (2007) Model-based methods of classification: using the mclust. J Stat Softw 18:1–13

Francois R, Altabet MA, Goericke R, McCorkle DC, Brunet C, Poisson A (1993) Changes in the $\delta^{13}C$ of surface water particulate organic matter across the subtropical convergence in the SW Indian Ocean. Global Biogeochem Cycles 7: 627–644

Hansen JH, Hedeholm RB, Sünksen K, Christensen JT, Grønkjær P (2012) Spatial variability of carbon ($\delta^{13}C$) and

nitrogen ($\delta^{15}N$) stable isotope ratios in an Arctic marine food web. Mar Ecol Prog Ser 467:47–59
Henschke N, Everett JD, Suthers IM, Smith JA, Hunt BPV, Doblin MA, Taylor MD (2015) Zooplankton trophic niches respond to different water types of the western Tasman Sea: a stable isotope analysis. Deep Sea Res I 104:1–8
Hirons AC, Schell DM, St. Aubin DJ (2001) Growth rates of vibrissae of harbor seals (*Phoca vitulina*) and Steller sea lions (*Eumetopias jubatus*). Can J Zool 79:1053–1061
Hobson KA, Piatt JF, Pitocchelli J, Piattt JF, Pitocchellij JAY (1994) Using stable isotopes to determine seabird trophic relationship. J Anim Ecol 63:786–798
Hückstädt LA, Koch PL, McDonald BI, Goebel ME, Crocker DE, Costa DP (2012) Stable isotope analyses reveal individual variability in the trophic ecology of a top marine predator, the southern elephant seal. Oecologia 169:395–406
Jeanniard-du-Dot T, Thomas AC, Cherel Y, Trites AW, Guinet C (2017) Combining hard-part and DNA analyses of scats with biologging and stable isotopes can reveal different diet compositions and feeding strategies within a fur seal population. Mar Ecol Prog Ser 584:1–16
Jenkins SG, Partridge ST, Stephenson TR, Farley SD, Robbins CT (2001) Nitrogen and carbon isotope fractionation between mothers, neonates, and nursing offspring. Oecologia 129:336–341
Kernaléguen L, Cazelles B, Arnould JP, Richard P, Guinet C, Cherel Y (2012) Long-term species, sexual and individual variations in foraging strategies of fur seals revealed by stable isotopes in whiskers. PLOS ONE 7:e32916
Kernaléguen L, Arnould JPYY, Guinet C, Cherel Y and others (2015) Determinants of individual foraging specialization in large marine vertebrates, the Antarctic and subantarctic fur seals. J Anim Ecol 84:1081–1091
Kroopnick PM (1985) The distribution of ^{13}C of ΣCO_2 in the world oceans. Deep Sea Res A, Oceanogr Res Pap 32:57–84
Lorrain A, Graham B, Menard F, Popp B, Bouillon S, van Breugel P, Cherel Y (2009) Nitrogen and carbon isotope values of individual amino acids: a tool to study foraging ecology of penguins in the Southern Ocean. Mar Ecol Prog Ser 391:293–306
Lowther AD, Harcourt RG, Page B, Goldsworthy SD (2013) Steady as he goes: at-sea movement of adult male Australian sea lions in a dynamic marine environment. PLOS ONE 8:e74348
McHuron EA, Walcott SM, Zeligs J, Skrovan S, Costa DP, Reichmuth C (2016) Whisker growth dynamics in two North Pacific pinnipeds: implications for determining foraging ecology from stable isotope analysis. Mar Ecol Prog Ser 554:213–224
McHuron EA, Holser RR, Costa DP (2019) What's in a whisker? Disentangling ecological and physiological isotopic signals. Rapid Commun Mass Spectrom 33:57–66
Middleton JF, Bye JAT (2007) A review of the shelf-slope circulation along Australia's southern shelves: Cape Leeuwin to Portland. Prog Oceanogr 75:1–41
Newland CB, Field IC, Cherel Y, Guinet C, Bradshaw CJA, McMahon CR, Hindell MA (2011) Diet of juvenile southern elephant seals reappraised by stable isotopes in whiskers. Mar Ecol Prog Ser 424:247–258
Newsome SD, Clementz MT, Koch PL (2010) Using stable isotope biogeochemistry to study marine mammal ecology. Mar Mamm Sci 26:509–572
Page B, McKenzie J, Goldsworthy SD (2005) Dietary resource partitioning among sympatric New Zealand and Australian fur seals. Mar Ecol Prog Ser 293:283–302
Peterson BJ, Fry B (1987) Stable isotopes in ecosystem studies. Annu Rev Ecol Syst 18:293–320
Pistorius P, Hindell M, Crawford R, Makhado A, Dyer B, Reisinger R (2017) At-sea distribution and habitat use in king penguins at sub-Antarctic Marion Island. Ecol Evol 7:3894–3903
R Core Team (2017) R: a language and environment for statistical computing. R Foundation for Statistical Computing, Vienna
Ramos R, González-Solís J (2012) Trace me if you can: the use of intrinsic biogeochemical markers in marine top predators. Front Ecol Environ 10:258–266
Rea LD, Christ AM, Hayden AB, Stegall VK and others (2015) Age-specific vibrissae growth rates: a tool for determining the timing of ecologically important events in Steller sea lions. Mar Mamm Sci 31:1213–1233
Reid K, Croxall JP (2001) Environmental response of upper trophic-level predators reveals a system change in an Antarctic marine ecosystem. Proc R Soc B 268:377–384
Rogers PJ, Ward T, van Ruth P, Williams A and others (2013) Physical processes, biodiversity and ecology of the Great Australian Bight region: a literature review. CSIRO Australia, Hobart
Ruiz-Cooley RI, Koch PL, Fiedler PC, McCarthy MD (2014) Carbon and nitrogen isotopes from top predator amino acids reveal rapidly shifting ocean biochemistry in the outer California current. PLOS ONE 9:e110355
Scherer RD, Doll AC, Rea LD, Christ AM and others (2015) Stable isotope values in pup vibrissae reveal geographic variation in diets of gestating Steller sea lions *Eumetopias jubatus*. Mar Ecol Prog Ser 527:261–274
Sumner MD (2016) Tools for the analysis of animal track data. https://github.com/Trackage/trip
Tomczak M, Pender L, Liefrink S (2004) Variability of the subtropical front in the Indian Ocean south of Australia. Ocean Dyn 54:506–519
Trueman CN, Mackenzie KM, Palmer MR (2012) Identifying migrations in marine fishes through stable-isotope analysis. J Fish Biol 81:826–847
Trull TW, Armand L (2001) Insights into Southern Ocean carbon export from the $\delta^{13}C$ of particles and dissolved inorganic carbon during the SOIREE iron release experiment. Deep Sea Res II 48:2655–2680
Tyrrell LP, Newsome SD, Fogel ML, Viens M, Bowden R, Murray MJ (2013) Vibrissae growth rates and trophic discrimination factors in captive southern sea otters (*Enhydra lutris nereis*). J Mammal 94:331–338
Vales DG, Cardona L, Garcia NA, Zenteno L, Crespo EA (2015) Ontogenetic dietary changes in male South American fur seals *Arctocephalus australis* in Patagonia. Mar Ecol Prog Ser 525:245–260
Waite AM, Pesant S, Griffin DA, Thompson PA, Holl CM (2007) Oceanography, primary production and dissolved inorganic nitrogen uptake in two Leeuwin Current eddies. Deep Sea Res II 54:981–1002
Walters A, Lea MA, van den Hoff J, Field IC and others (2014) Spatially explicit estimates of prey consumption reveal a new krill predator in the Southern Ocean. PLOS ONE 9:e86452

Editorial responsibility: Yves Cherel, Villiers-en-Bois, France

Submitted: April 26, 2019; Accepted: August 23, 2019
Proofs received from author(s): October 7, 2019